Influence of viscosity, binder activation, and loading rate on the membrane response of an infiltrated UD-NCF

MIRANDA PORTELA Renan[1,a] *, SCHÄFER Bastian[2,b], KÄRGER Luise[2,c], ROCHA DE FARIA Alfredo[3,d], and MONTESANO John[1,e]

[1]Composites Research Group, Department of Mechanical & Mechatronics Engineering, University of Waterloo, Waterloo, Canada

[2]Karlsruhe Institute of Technology (KIT), Institute of Vehicle System Technology (FAST), Karlsruhe, Germany

[3]Department of Mechanical Engineering, Instituto Tecnológico de Aeronáutica (ITA), São José dos Campos, Brazil

[a]renan.portela@uwaterloo.ca, [b]bastian.schaefer@kit.edu, [c]luise.kaerger@kit.edu, [d]arfaria@ita.br, [e]john.montesano@uwaterloo.ca

Keywords: Infiltrated Bias Extension Tests, Experimental Characterization, UD-NCF

Abstract. Shear-tension coupling of engineering fabric is one of the most important behaviors during the draping phase of liquid composite molding (LCM) processes, including wet compression molding (WCM), which occurs with the infiltrated fabric and, in some cases, with the use of a stabilizing binder. In the present study, the membrane behavior of an impregnated and binder-stabilized uni-directional carbon fiber non-crimp fabric was characterized by performing off-axis tension tests. These tests allow the investigation of the influence of stabilizing binder, fluid viscosity and loading rate on the fabric membrane behavior. As result of these experimental tests, an increase in membrane force is noticed when the stabilizing binder is activated, attributed to a greater shear stiffness. Additionally, a decrease in forces is observed for impregnated fabric compared to dry textiles caused by a lubrication layer between fiber tows. The study provides a better understanding of the membrane behavior of the impregnated and binder-stabilized UD-NCF, which is relevant for a potential high-volume production process.

Introduction

Automated wet compression molding (WCM) with fast-curing resin enables high-capacity production of continuous fiber-reinforced composite components [1]. The WCM process involves four simultaneously occurring physical mechanisms, which includes viscous draping, fluid progression, non-isothermal curing, and strong fluid-structure interaction [2]. Viscous draping of the fabric layers during mold closure is an inherent characteristic of the WCM process, involving complex mechanisms such as bending and membrane deformation, layer compaction, and frictions between adjacent layers and between layer and tool [2], [3]. During engineering textile draping process, membrane deformation is critical, as it can directly influence the formation of defects and misalignment of fibers [4], [5]. For the WCM process, membrane deformation may be influenced by the varying resin viscosity within the mold and the deformation rate.

Unidirectional non-crimp fabrics (UD-NCF) have been increasingly used in structural applications and, in some cases, are preferred over more conventional woven fabrics. UD-NCFs comprise parallel-oriented reinforcing fiber tows and low density transversely oriented supporting fibers held together by stitching thread, providing stability during the handling and manufacturing process. Unlike woven fabrics, UD-NCFs have no tow interlacing, minimizing tow crimp and, as a result, increasing the in-plane mechanical properties of fabricated composite parts [5]–[9]. However, the elimination of tow interlacing leads to lower fabric handleability, which may affect

the manufacturing automation and process time [10]. The addition of a stabilizing binder can improve the handling of UD-NCFs by providing higher cohesion between adjacent layers and mitigating ply slippage, while potentially reducing the manufacturing cost [5], [10]. For thick WCM parts with complex geometries, binder stabilized UD-NCFs may aid in increasing the fabric stack stiffness for improved resin management prior to mold closure. For binder stabilized UD-NCFs, the pre-activation of the binder may further influence the membrane deformation.

In general, membrane deformation is measured either by picture frame test (PFT) or bias-extension test (BET) setups [11], [12]. The PFT works by applying uniaxial tensile forces to the low and top corners of the testing frame. It is conducted with a testing frame, initially in a square shape. During the experimental test, the testing frame deforms into a rhomboid while simultaneously imposing pure shear stress on the fabric sample. PFTs have been used for characterizing the shear deformation of woven fabrics due to their balanced nature [4], [13]. However, PFTs are not suitable for the characterization of UD-NCFs due to the fabric behavior that combines pure and simple shear [14], [15]. These two shear mechanisms are represented by the rotation and slippage of the fiber tows, respectively [14]. On the other hand, BET is performed with a rectangular shape fabric specimen that must have length to width ratio greater than 2. This type of test can be used to measure the extension-shear behavior with the fabric oriented in different directions, such as $30^o, 45^o$, and 60°. In Ref [16], the authors indicated that 45° BET can be used to capture the UD-NCF shear response, while other studies suggest that 30° and 60° BET provide a more comprehensive understanding of the UD-NCF behavior [12], [14], [15].

Both the PFT and BET are suitable to characterize the membrane deformation of dry fabric. In Refs. [1], [2], an infiltrated bias-extension test (IBET) setup was designed to characterize the extension-shear deformation of impregnated woven fabric, which is representative of fabric draping during the WCM process. The IBET requires a horizontal frame with a reservoir, a rear fixture that holds the fabric, and a moving bridge that extends the engineering textile. In the reservoir, an amount of silicone oil is poured to fully impregnate the fabric before the test. Although impregnated woven fabrics were characterized in previous work [1], [2], the extension-shear behavior of impregnated UD-NCFs has not been studied. Furthermore, the influence of binder activation on the membrane deformation of UD-NCFs has not been studied.

In this work, the shear-tension behavior of an impregnated and binder stabilized carbon fiber UD-NCF is investigated through a series of IBETs. Thereby, the influence of the loading rate, fluid viscosity, and activation of binder on the membrane deformation response is investigated.

Experimental Procedure
Materials. A binder stabilized UD-NCF (Figure 1) was investigated, namely PX35-UD300 (Zoltek, US). This fabric consists of a single layer of axially oriented parallel tows each comprising 50K continuous PX35 carbon fibers (CFs) stitched together with a 76 dtex polyester yarn in a tricot pattern. The fabric also consists of transversely oriented low linear density supporting glass fibers (GF) for improved handleability and a thermosetting polymer powder binder applied on one surface. The total areal density of the UD-NCF is 333 g/m². To impregnate the textiles and avoid additional temperature-related uncertainties, silicone oils with two different viscosities (20 and 100 cSt) were used.
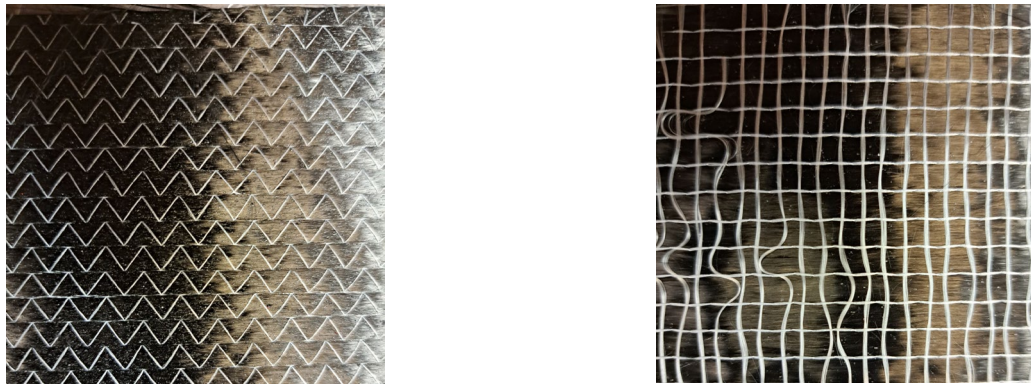
Figure 1: Binder stabilized uni-directional non-crimp fabric (PX35-UD300); left: Polyester stitching yarns in a tricot pattern; right: Glass fiber to improve the fabric handleability.

Infiltrated bias-extension test (IBET) The IBET was performed on a servo-hydraulic test frame within the same fixture used by Poppe et al. [1], comprising a reservoir, a moving bridge attached to a $1\ mm$ wire and a rear fixture as illustrated in Figure 2. When the IBET is conducted, the moving bridge is pulled, and the specimen, attached to both fixtures, is stretched. This setup was mounted on a servo-hydraulic test frame with a $1\ kN$ load cell. Undeformed layers with a size of $280 \times 140\ mm^2$ and two different bias angles (30° and 60°) were tested at different loading rates of 100 and $500\ mm/min$, under both dry and infiltrated conditions with two different liquid viscosities ($20\ cSt$ and $100\ cSt$), and with the binder pre-activated and inactivated. Each test was performed three times with a new UD-NCF specimen.
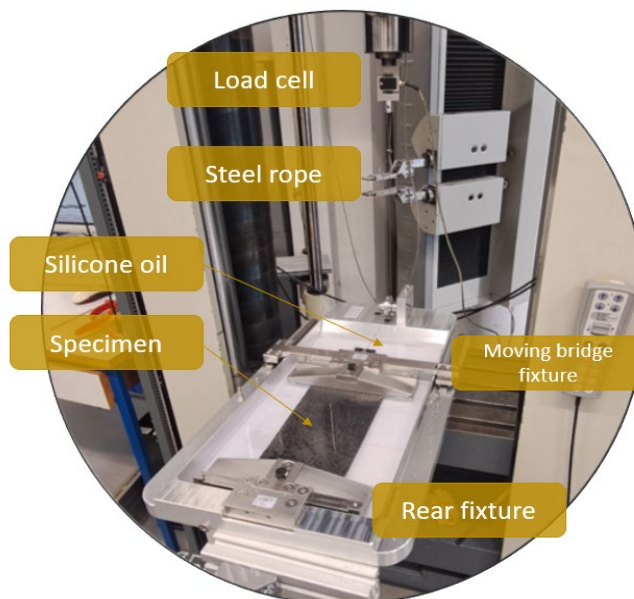
Figure 2: Experimental IBET setup.

Similar to the evaluation methodology proposed by Poppe et al. [1], the shear resulting forces (f_{shear}) were found by:

$$f_{\text{shear}} = f_{\text{raw}} - f_{\text{friction}} - f_{\text{fluid}}(v, \mu) \qquad (1)$$

where f_{raw} is the force measured by the universal testing machine, f_{friction} is the frictional force within the linear bearings, and $f_{\text{fluid}}(v, \mu)$ is the fluid resistance on the moving, which is expressed as a function of fluid viscosity (μ) and loading rate or velocity (v). The last two forces were

determined by performing the IBET with no specimen. For each configuration of viscosity and velocity, calibration tests were conducted 5 times.

Results and Discussion

Influence of fluid viscosity. To investigate the influence of the fluid viscosity, two different fabric orientations (30° and 60°) were tested, both dry and impregnated with two different fluid viscosities (20 and 100 cSt). The displacement fields of both fabric orientations are illustrated in Figure 3. The results for the 30°-IBET and 60°-IBET are shown in Figure 4 and 5, respectively. For both considered fluid viscosities in the 30°-IBET, the average force of the dry specimens was up to 30% higher at the final displacement of approximately $50\ mm$ (Figure 4). When the fabric is impregnated, it is observed a membrane force reduction, which is attributed to a lower friction between fibers within the tow and between the fiber tows and the stitching, resulting from the lubrication layer on the fibers tows [1]. The same phenomenon occurs for an initial orientation of 60°, cf. Figure 5 (right), where the dry specimen has a higher membrane force. This force is reduced when the specimen is impregnated. On the other hand, an anomaly was observed in Figure 5 (left), showing higher membrane forces in the infiltrated specimens with $100\ cSt$ compared to the dry specimens. This may be due to slippage of the sample during the experiment.
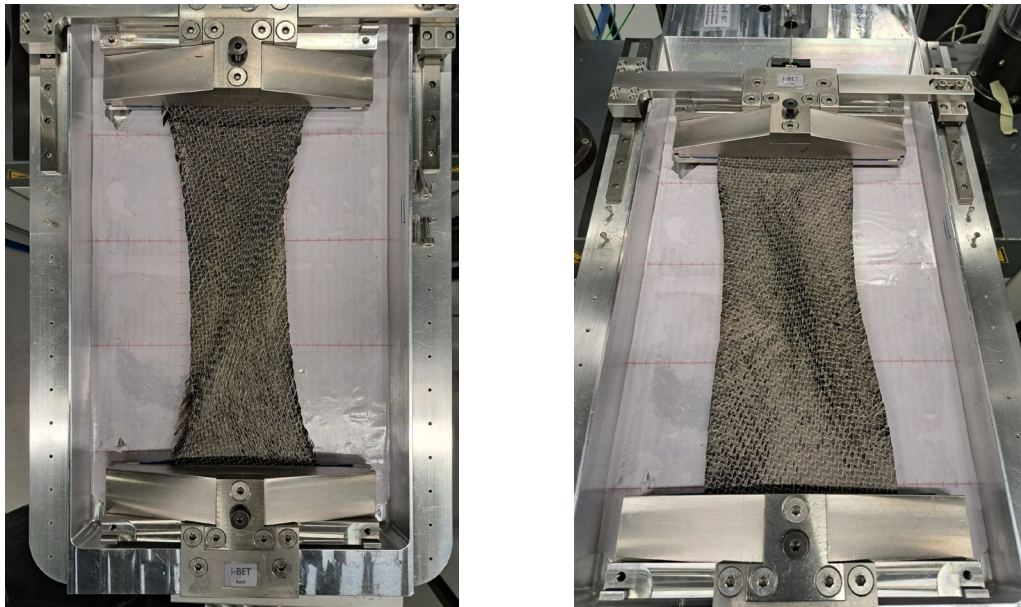
Figure 3: UD-NCF deformation field; left: 30° *test specimen; right:* 60° *test specimen.*
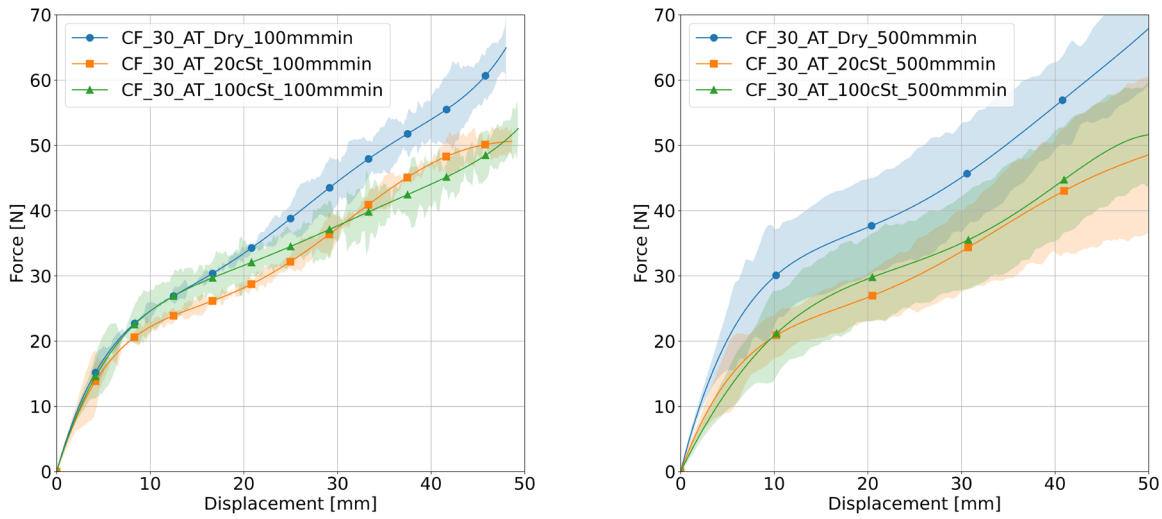
Figure 4: Experimental results for dry (blue) and impregnate (20 cSt in orange and 100 cSt in green) UD-NCF specimens; left: 30° *specimens tested at 100 mm/min; right:* 30° *specimens tested at 500 mm/min.*
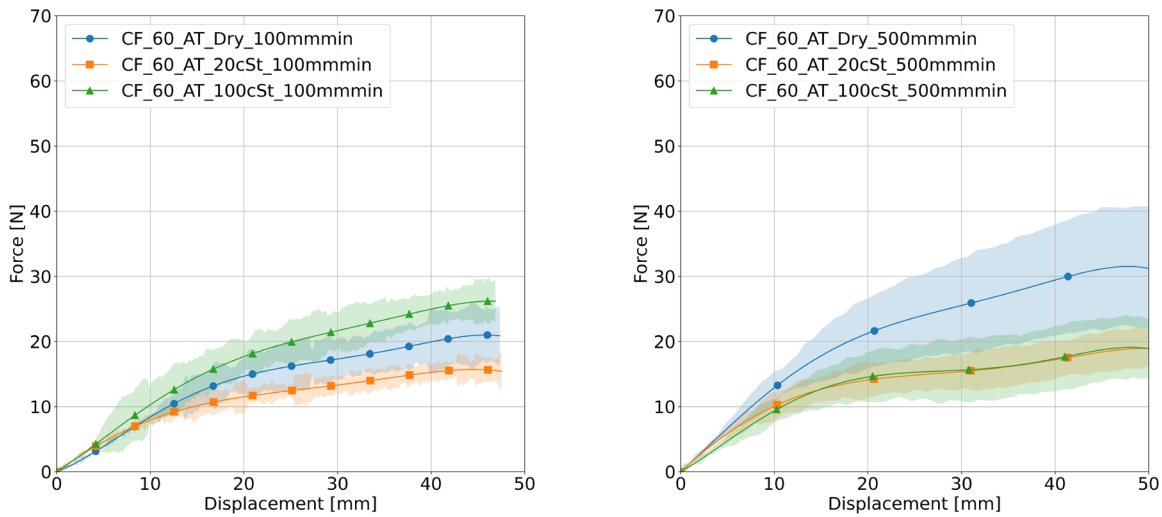
Figure 5: Experimental results for dry (blue) and impregnated (20 cSt in orange and 100 cSt in green) UD-NCF specimens; left: 60° *specimens tested at 100 mm/min; right:* 60° *specimens tested at 500 mm/min.*

Influence of fabric binder pre-activation. Figure 6 presents the fabric with inactivated binder (left) and the pre-activated binder (right). Figure 6 (left) shows the presence of polymer grains, which are pulverized over the fabric surface by the material supplier during the textile manufacturing process. When the binder is pre-activated in the oven at $120\,°C$, these grains melt and coat the nearest fibers and stitching. Figures 7 and 8 illustrate the influence of the pre-activated binder on the membrane force of the fabric initially oriented at 30° and 60°, respectively. The configurations with pre-activated binder are denoted by AT and without pre-activation of the binder as IT. The membrane force increases as the stabilizing binder is activated. This is due to the polymer binder

that melts and coats the fiber tows and additionally increases cohesion between the tows and the stitching. This increases the shear stiffness of the fabric. In some cases, this phenomenon increases the membrane force up to 100% at different displacement values, including $20\ mm$ and $40\ mm$, as shown in Figure 8 (right).

Figure 6: Binder-stabilized UD-NCF; left: Inactivated binder; right: Pre-activated binder in the oven at $120\ °C$.
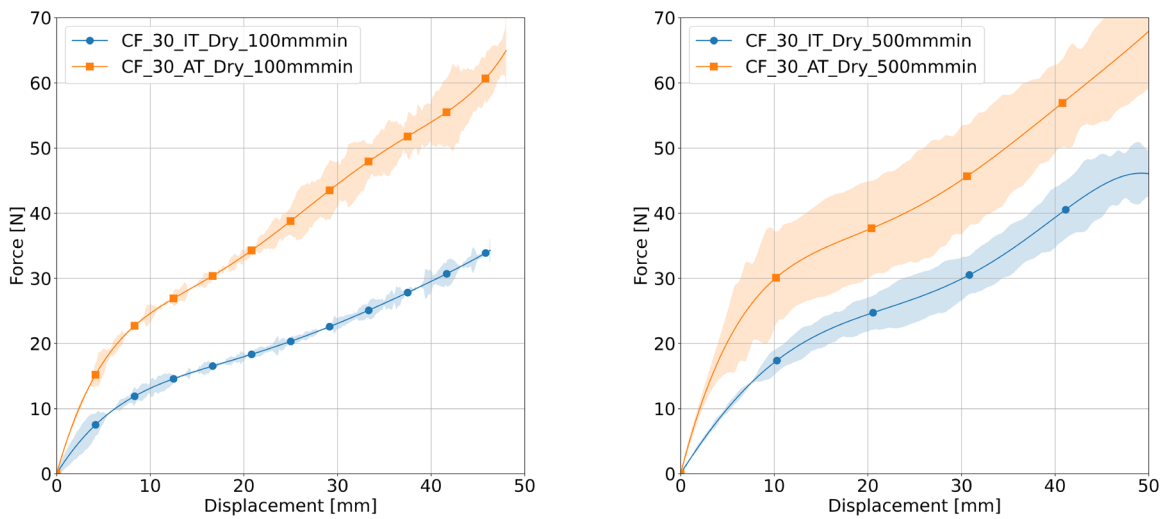
Figure 7: Experimental results for dry inactivated (IT) and pre-activated (AT) binder on the UD-NCF specimens; left: 30° specimens tested at 100 mm/min; right: 30° specimens tested at 500 mm/min.
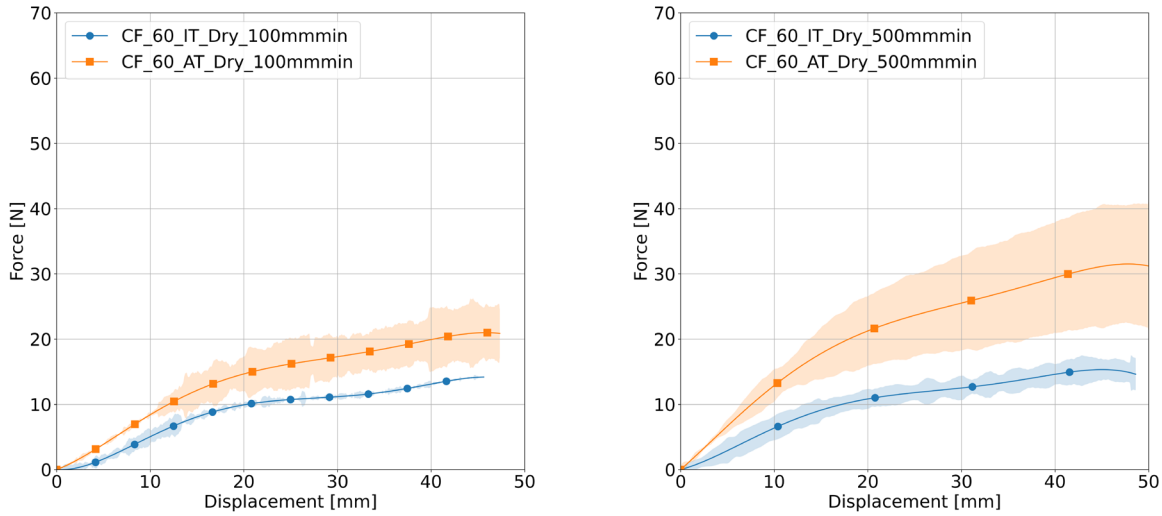
Figure 8: Experimental results for dry inactivated (IT) and pre-activated (AT) binder on the UD-NCF specimens; left: 60° *specimens tested at 100 mm/min; right:* 60° *specimens tested at 500 mm/min.*

Influence of loading rate. To understand the influence of the loading rate, the specimens were tested at two different rates. The 30°- and 60°-IBET specimens, presented in Figures 9 and 10, respectively, were tested under 100 and 500 $\frac{mm}{min}$. Figure 9 illustrates the results of the 30° specimens that overlap regardless of the infiltration state of the fabric, which means that for this orientation the loading rate has no influence over the membrane force. The results of the 60°-IBET specimens show an increase of the average membrane force when the specimens were dry (Figure 10 left); however, the standard deviation of both loading rates overlap, representing no significant difference between both loading rates. Analogously, the results of the infiltrated samples with 20 *cSt* silicone oil are similar, indicating no influence of the loading rate on the membrane force. Lastly, a higher membrane force was obtained at a slower loading rate when the specimens were infiltrated with 100 *cSt* silicone oil. The 60° bias angle is more complex because of the possible slippage of the specimen which can have affected the results presented in Figure 10 right.
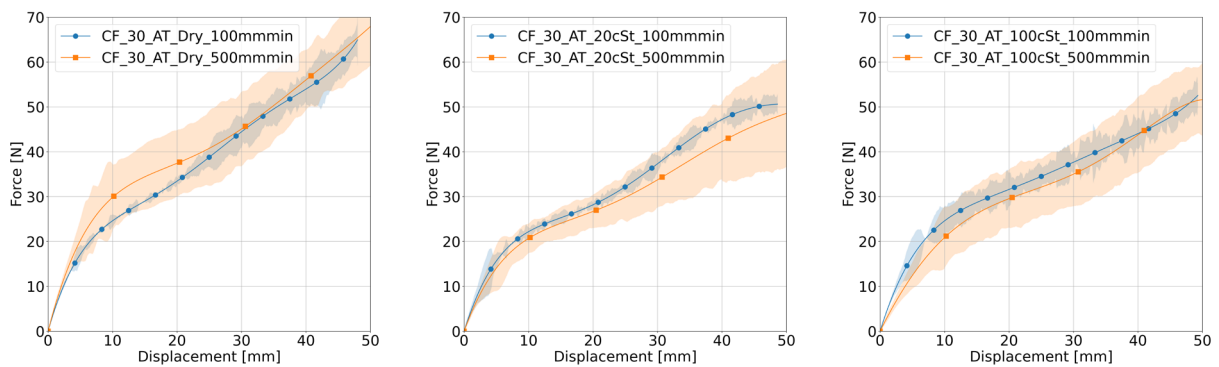
Figure 9: Experimental results for dry and impregnated UD-NCF specimens with activated binder system (AT); left: dry 30° *specimens tested at 100 and 500 mm/min; center: impregnated* 30° *specimens under 20 cSt tested at 100 and 500 mm/min; right: impregnated* 30° *specimens under 100 cSt tested at 100 and 500 mm/min.*
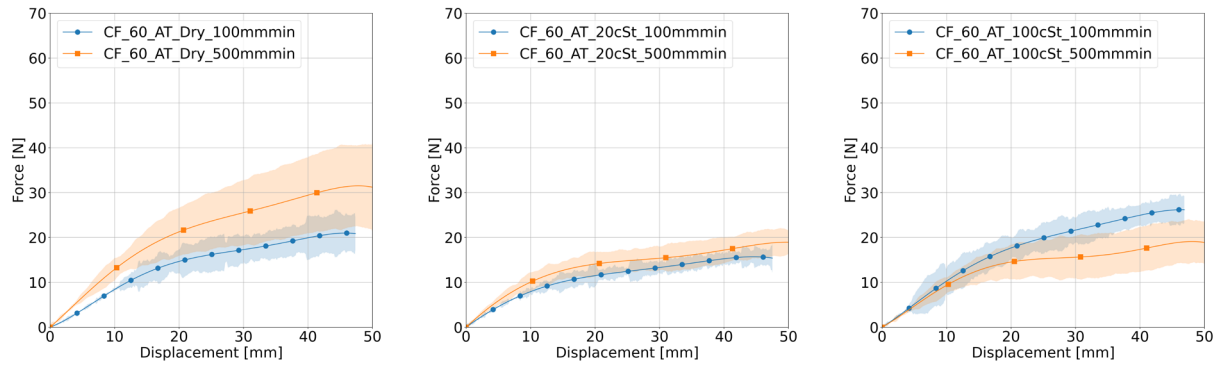
Figure 10: Experimental results for dry and impregnated UD-NCF specimens with activated binder system (AT); left: dry 60° specimens tested at 100 and 500 mm/min; center: impregnated 60° specimens under 20 cSt tested at 100 and 500 mm/min; right: impregnated 60° specimens under 100 cSt tested at 100 and 500 mm/min.

Summary and conclusion

In conclusion, the binder activation causes an increase of the fabric's membrane stiffness. The increase of the membrane stiffness happens because of the polymer binder that melts and, consequently, coats the fiber tows and increases cohesion with the stitching, increasing the fabric's membrane stiffness. On the other hand, the fluid viscosity creates a lubrication layer between the fiber tows and the stitching, reducing the friction, and consequently, decreasing the membrane stiffness. At last, no significant influence of the strain rate on the 30°- and 60°-IBET specimen results was found.

References

[1] C. Poppe, D. Dörr, F. Henning, and L. Kärger, "Experimental and numerical investigation of the shear behaviour of infiltrated woven fabrics," *Compos. Part A Appl. Sci. Manuf.*, vol. 114, pp. 327–337, Nov. 2018. https://doi.org/10.1016/j.compositesa.2018.08.018

[2] C. Poppe, "Process simulation of wet compression moulding for continuous fibre-reinforced polymers," Karlsruhe Institute of Technology, Karlsruhe, 2021.

[3] C. T. Poppe, C. Krauß, F. Albrecht, and L. Kärger, "A 3D process simulation model for wet compression moulding," *Compos. Part A Appl. Sci. Manuf.*, vol. 145, p. 106379, 2021. https://doi.org/10.1016/j.compositesa.2021.106379

[4] M. Ghazimoradi, E. A. Trejo, C. Butcher, and J. Montesano, "Characterizing the macroscopic response and local deformation mechanisms of a unidirectional non-crimp fabric," *Compos. Part A Appl. Sci. Manuf.*, vol. 156, p. 106857, May 2022. https://doi.org/10.1016/j.compositesa.2022.106857

[5] J. Pourtier, B. Duchamp, M. Kowalski, X. Legrand, P. Wang, and D. Soulat, "Bias extension test on a bi-axial non-crimp fabric powdered with a non-reactive binder system," in *AIP Conference Proceedings*, 2018, vol. 1960, p. 020023. https://doi.org/10.1063/1.5034824

[6] S. V. Lomov, *Non-crimp fabric composites*. Cambridge, UK: Woodhead Publishing Limited, 2011. https://doi.org/10.1533/9780857092533

[7] B. Schäfer, R. Zheng, P. Boisse, and L. Kärger, "Investigation of the compaction behavior of uni-and bidirectional non-crimp fabrics," in *Materials Research Proceedings*, 2023, vol. 28, pp. 331–338. https://doi.org/10.21741/9781644902479-36

[8] P. Quenzel *et al.*, "Material characterisation of biaxial glass-fibre non-crimp fabrics as a function of ply orientation, stitch pattern, stitch length and stitch tension," *J. Compos. Mater.*, vol. 56, no. 26, pp. 3971–3991, Nov. 2022. https://doi.org/10.1177/00219983221127005

[9] L. Kärger, S. Galkin, E. Kunze, M. Gude, and B. Schäfer, "Prediction of forming effects in UD-NCF by macroscopic forming simulation – Capabilities and limitations," in *ESAFORM 2021*, 2021, pp. 14–16. https://doi.org/10.25518/esaform21.355

[10] P. H. Broberg, C. Krogh, E. Lindgaard, and B. L. V. Bak, "Simulation of Wrinkling during Forming of Binder Stabilized UD-NCF Preforms in Wind Turbine Blade Manufacturing," *Key Eng. Mater.*, vol. 926, pp. 1248–1256, Jul. 2022. https://doi.org/10.4028/p-165q46

[11] P. Boisse, N. Hamila, E. Guzman-Maldonado, A. Madeo, G. Hivet, and F. Dell'Isola, "The bias-extension test for the analysis of in-plane shear properties of textile composite reinforcements and prepregs: a review," *Int. J. Mater. Form.*, vol. 10, no. 4, pp. 473–492, Aug. 2017. https://doi.org/10.1007/s12289-016-1294-7

[12] F. J. Schirmaier, D. Dörr, F. Henning, and L. Kärger, "A macroscopic approach to simulate the forming behaviour of stitched unidirectional non-crimp fabrics (UD-NCF)," *Compos. Part A Appl. Sci. Manuf.*, vol. 102, pp. 322–335, Nov. 2017. https://doi.org/10.1016/j.compositesa.2017.08.009

[13] G. Barbagallo, A. Madeo, I. Azehaf, I. Giorgio, F. Morestin, and P. Boisse, "Bias extension test on an unbalanced woven composite reinforcement: Experiments and modeling via a second-gradient continuum approach," *J. Compos. Mater.*, vol. 51, no. 2, pp. 153–170, Jan. 2017. https://doi.org/10.1177/0021998316643577

[14] B. Schäfer, R. Zheng, N. Naouar, and L. Kärger, "Membrane behavior of uni- and bidirectional non-crimp fabrics in off-axis-tension tests," *Int. J. Mater. Form.*, vol. 16, no. 6, pp. 16–20, 2023. https://doi.org/10.1007/s12289-023-01792-x

[15] F. J. Schirmaier, K. A. Weidenmann, L. Kärger, and F. Henning, "Characterisation of the draping behaviour of unidirectional non-crimp fabrics (UD-NCF)," *Compos. Part A Appl. Sci. Manuf.*, vol. 80, pp. 28–38, Jan. 2016. https://doi.org/10.1016/j.compositesa.2015.10.004

[16] M. Ghazimoradi and J. Montesano, "Macroscopic Forming Simulation for a Unidirectional Non-crimp Fabric Using an Anisotropic Hyperelastic Material Model," *Appl. Compos. Mater.*, vol. 30, no. 6, pp. 2001–2023, Dec. 2023. https://doi.org/10.1007/s10443-023-10158-0